

LABORATORY AND NUMERICAL STUDIES OF HYDRODYNAMICS NEAR JETTIES

ZEKI DEMIRBILEK*, LIHWA LIN and WILLIAM C. SEABERGH

*U.S. Army Engineer R&D Center,
3909 Halls Ferry Road, Vicksburg, MS, 39180, USA*

** Tel: 601-634-2834; Fax: 601-634-3433*

** zeki.demirbilek@usace.army.mil*

HAJIME MASE

*Disaster Prevention Research Institute,
Kyoto University, Gokasho, Uji, Kyoto 611-0011, Japan*

JINHAI ZHENG

*Research Institute of Coastal & Ocean Engineering,
Hohai University, Nanjing 210098, China*

Received 24 March 2008

Revised 6 February 2009

Numerical and physical modeling studies were performed by the Coastal Inlets Research Program (CIRP) of the U.S. Army Corps of Engineers to investigate the spatial and temporal behavior of waves and wave-induced currents near jetties of an idealized coastal inlet. Hydrodynamics were examined in the vicinity of two extreme types of jetty structure: a highly absorbing jetty (resembling fairly porous rock rubble structure) and a fully reflective jetty (resembling a vertical sheet pile or caisson type breakwater). Laboratory experiments in a Froude scale of 1:50 were conducted with regular and irregular shore-normal (0°) and obliquely incident (20°) unidirectional waves. Current and wave measurements were made on the up-wave side and inside the inlet as well as in the bay, along a number of cross-shore and along-shore transects. Wave directions were measured by a remote-sensing video-camera system and Acoustic Doppler Velocimeters (ADV). Numerical modeling was performed with the Coastal Modeling System (CMS) consisting of a two-dimensional circulation model coupled to a spectral wave model. Calculated current and wave fields from CMS in the area around and between absorbing or reflected jetties were compared to measurements. The highly reflecting jetty created a circulation cell on the up-wave side of the inlet, whereas the absorbing jetty did not.

*Corresponding author.

Keywords: Coastal inlet; laboratory wave measurements; numerical models; wave-induced currents; jetties.

1. Introduction

Waves approaching a coastal inlet can refract, diffract, and shoal as they travel from deeper water toward the vicinity of an inlet, and eventually break nearshore creating a longshore current that interacts with the tidal current at the inlet. Waves and currents are a primary concern in the operation and maintenance of navigation channels. Wave attack on a protective jetty or breakwater of a navigable inlet can create complex circulation patterns adjacent to and inside the inlet. The resulting sediment transport at inlets can cause channel erosion, deposition, and navigation hazards. The combined wave-current processes at coastal inlets determine navigation risk, frequency of dredging requirements for the channel maintenance, repair of inlet structures, and extent of channel sedimentation and morphology change. Accurate and reliable prediction of currents and waves is paramount for safe navigation through inlets into bays and commercial harbors.

The U.S. Army Corp of Engineers (USACE) designs and maintains entrance jetties, breakwaters, training structures, and other types of coastal structures in support of federal navigation projects. These structures constrain currents that can scour navigation channels, stabilize the location of channels and entrances, and provide wave protection to vessels transiting through inlets into harbors. Numerical wave predictions are frequently sought for rehabilitating or improving navigation structures that degrade during their life-cycle. The USACE Districts are required to develop long-range plans to manage navigation structures, build and maintain jetties at inlets to improve navigability and reduce channel sedimentation. On the sea side of an inlet, breaking waves generate currents that typically flow along the shore until diverted seaward by irregular bathymetry or a jetty. These longshore currents can carry sediment into the inlet, and create strong cross-currents across the navigation channel, both of which can significantly degrade safety of navigation.

Flow patterns at inlets based on physical, analytical, and numerical models were discussed by Seabergh [1988]. Data collection from physical models was limited at the time to using dye to measure current fields because the inertia of mechanical current meters precluded accurate measurements. Reliable laboratory current measurements have been reported [Seabergh and Smith, 2001] using Acoustic-Doppler type velocimeters (ADVs). Using similar instruments, Osborne [2003] and Sherwood *et al.* [2001] have measured field currents in a high-energy prototype environment on the ebb shoal and adjacent regions near jetties at Grays Harbor, WA.

Although physical modeling has been the primary means used by the USACE for evaluating the complex dynamics of coastal inlets and navigation projects, advanced numerical models have been developed in recent years for predicting circulation, waves, and morphodynamics at coastal inlets and adjacent beaches. The CMS is

a suite of coupled models developed specifically for coastal inlet applications that consists of two-dimensional (2D) and three-dimensional (3D) hydrodynamic models [Buttolph *et al.*, 2006], wave models [Mase *et al.*, 2005; Lin *et al.*, 2006; Demirbilek *et al.*, 2007; Lin *et al.*, 2008], and sediment transport models [Camenen and Larson, 2007]. The reader is referred to references about other models for inlets, structures, navigation and harbors [e.g. Isobe, 1998; Panchang and Demirbilek, 1998; Yu *et al.*, 2000; Nwogu and Demirbilek, 2001; Holthuijsen *et al.*, 2004]. Grunnet *et al.* [2004] have described a systematic approach for validation of 2D and 3D hydrodynamic models for the nourishment of beaches adjacent to coastal inlets using temporally and spatially varying data. Near-jetty hydrodynamics may require 3D models to represent the complex flow patterns developing adjacent to the structures.

In collaboration with researchers at Kyoto University, Japan, the CIRP has developed a numerical model for spectral wave transformation to address the needs of USACE navigation projects [Mase and Kitano, 2001; Mase, 2001; Mase *et al.*, 2005; Lin *et al.*, 2006; Demirbilek *et al.*, 2007; Lin *et al.*, 2008]. This model is CMS-Wave, previously known as WABED (Wave-Action Balance Equation with Diffraction). It is operated within the Surface-water Modeling System (SMS), an interactive and comprehensive graphical user interface environment for preparing model input, running models, and viewing and analyzing numerical model results (<http://www.xmswiki.com>). CMS-Wave is designed specifically for wave processes affecting operation and maintenance of coastal inlet structures, navigation projects, and for risk assessment of ships moving through navigation channels and harbors. Nearshore wave processes considered in the CMS-Wave include wave shoaling, refraction, diffraction, reflection, wave breaking and dissipation mechanisms, wave-current interaction, wave generation, wave setup and wave overtopping structures. In CMS, both current and wave models can run in the coupled mode to calculate combined current-wave effects on the hydrodynamics, forcing on structures, sediment transport, morphology change in the navigation channels and inlets.

Two physical modeling experiments are described in this paper. These experiments were conducted to obtain current and wave data around jetties of simple inlet configurations for investigating basic inlet processes and validating numerical models. In the first physical model study, wave height and direction were measured behind a detached breakwater, a dogleg jetty, and in an inlet-bay system [Seabergh *et al.*, 2002]. These data have been used by Lin and Demirbilek [2005] in the evaluation of two steady-state spectral wave models. In the second laboratory experiment, both waves and currents were measured around jetties and inside inlets [Seabergh *et al.*, 2005a, 2005b, 2007]. Measurements were made along several cross-shore and alongshore transects on the sea and bay sides of an inlet, and inside the inlet between two jetties. Results of numerical simulations are compared with laboratory data to determine the efficacy of the CMS for calculating the combined hydrodynamics (waves plus currents) at coastal inlets. The physical model experiments are described in Sec. 2, and numerical modeling and comparison to measurements in

Sec. 3. Numerical model performance is analyzed in Sec. 4, and conclusions are given in Sec. 5.

2. Physical Modeling Studies

2.1. *Laboratory facility description*

Prior to constructing the laboratory model facility in early 1990s, important physical characteristics of approximately 100 USA federal tidal inlets were assembled into a database and analyzed. The goal was to design an idealized inlet model to study inlet hydrodynamic processes (waves, currents, sediment transport, etc.). The model parameters for the idealized inlet (channel depth, minimum width, average bay depth, bay surface area, offshore beach slope, etc.) were determined from the database. The equivalent prototype represents a typical U.S. east coast inlet. A model scale of 1:50 was selected based on the available facility, and this model scale was used and verified in prior inlet physical modeling studies. The foreshore slope was based on Dean's equilibrium profile (with the scale coefficient $A = 0.24$) to ensure a relatively steep beach (from -5 to 0 m) able to create strong wave breaking, circulation, and sedimentation. These features of idealized inlet model allow numerical modelers to evaluate capabilities of inlet wave and flow models. Different types of inlet structures (jetties, breakwaters, spurs, etc) may be added to and used with this model. In the present study, only fully reflective and absorbing structures were considered. Structures with partial reflection such as rubble-mound breakwaters will be investigated in subsequent studies.

An idealized inlet was designed within a 46-m wide by 99-m-long concrete basin with 0.6 m high walls. Figure 1 shows the facility and basin area. A 1:50 undistorted Froude model scale was used to represent the dimensions of a medium-sized Atlantic coast inlet of the United States. The equivalent full-scale (prototype) inlet dimensions were: the seaward prototype depth was 15 m at the wave generator, contours started 9.1 m from the generators with a 1/50 slope and transitioned shoreward to a steeper slope based on the equilibrium beach profile (with the scale coefficient $A = 0.24$). Experiments were conducted with 1.5 m water level above the mean low water datum. Average inlet width was 133 m, the depth at the middle of inlet throat was 7.6 m, and the depth of bay side floor connecting to the inlet was constant (6.1 m).

Fully reflective and fully absorbing jetties were constructed for inlet geometries studied. This choice of simple structures avoids difficulties of determining partial reflection, absorption of energy into and wave runup/run-down over rubble-mound structures, and allows modelers to objectively assess reliability of the calculated waves and flows near inlet structures. Numerical models exhibited significant spatial and temporal changes in wave and flow processes in different areas of inlets. The fundamental question was not how well the physical model could simulate the real world because previous studies have shown it working successfully at this scale

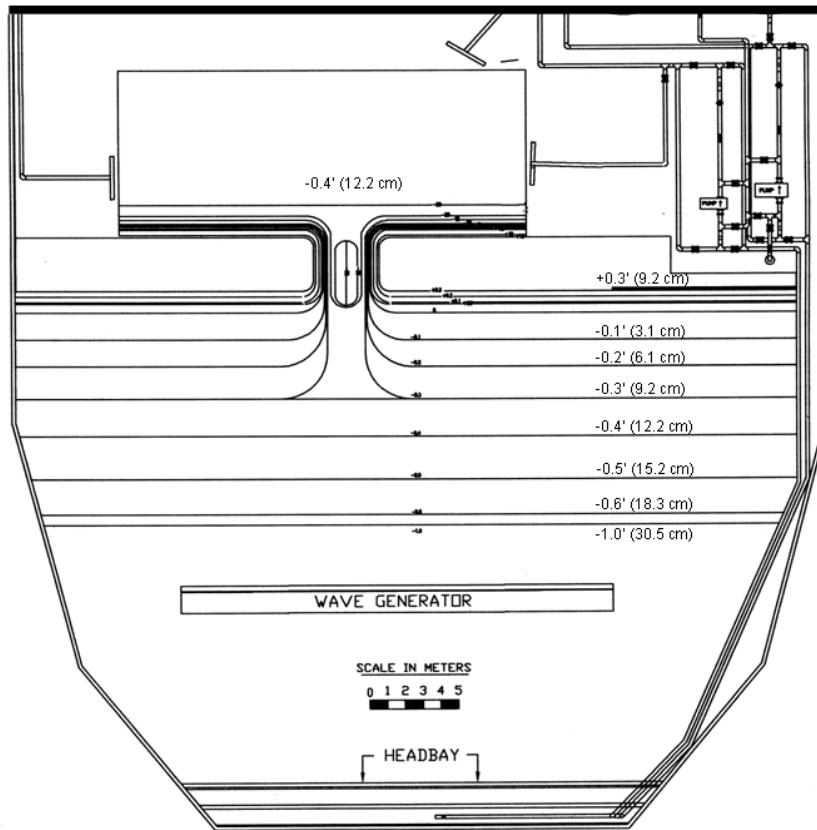


Fig. 1. Idealized inlet model research facility.

[Seabergh, 1988, 1999; Seabergh and Smith, 2001; Seabergh *et al.*, 2002]. The real question was how well could numerical models reproduce the physical model results for different types of inlet geometries. It was comforting to find out that numerical model results consistently followed the trend of data for all inlet geometries investigated. This outcome could have been different if the structures studied were not fully reflective or fully absorbing. With the chosen structures, it became possible to objectively evaluate numerical models without guessing values of reflection coefficients. Rubble-mound structures with reflection between $R = 0$ and $R = 1$ will be tested in the next study.

Steady ebb/flood currents were generated with a piping/pump system [Seabergh, 1999]. An adjustable (moving and rotating) 24 m-long plunger-type wave generator produced regular or irregular unidirectional waves up to 5 m in height (full-scale or prototype). Wave signal generation and data acquisition were controlled by a personal computer system. Wave height and period data were obtained with electrical capacitance wave gauges. The gauges were calibrated daily with a computer-controlled procedure that incorporates a least square fit of measurements

at 11 steps of gauge elevation. This averaging technique, using 21 voltage samples per gauge, minimizes the errors from slack in the gear drives and any hysteresis in the sensors. Typical calibration errors are less than 1 percent of full scale for the capacitance wave gauges, resulting in measurements accurate to 0.3 mm in the laboratory.

Velocity data were collected with SonTek 2D Acoustic Doppler Velocimeters (ADV) with a side-looking probe that is oriented to collect x - y horizontal velocity information in a horizontal plane. Samples were collected at 20 Hz for 10 minutes (i.e. 12,000 data points). Accuracy is 0.5 percent of the measured velocity, with resolution of 0.1 mm/s and threshold of 0.1 cm/sec. The probe samples a 0.25 cm³ water volume located 5 cm from the sensor heads. The wave height and velocity measurements were 600-sec-long records of transient data segments. Approximately 100 sec was required to reach steady state in tests done with smaller waves (1 m height and 11 sec period in full-scale). Larger waves (e.g. 2 m height and 11 sec period) required a longer time, up to 200 sec, to reach steady state. Current measurements required similar steady-state setup times as those for waves. Curtis *et al.* [2001 & 2002], and Seabergh *et al.* [2005a & 2005b] provide details of physical model components, instrumentation accuracy, measurement errors, and data analysis.

2.2. Phase I experiments

Four idealized inlet configurations with the following structures were tested: a shore-parallel semi-infinite offshore breakwater ($S1$), a dogleg jetty ($S2$), two equal-width barrier islands without stabilizing jetties ($S3$), and a dual-jetty inlet ($S4$). For instance, the inlet configuration $S4$ is depicted in Fig. 2(a), and sketches of other inlet geometries are shown in Figs. 3, 4, 7 and 11. The reader is referred to Seabergh *et al.* [2002] for a detailed description of the experiments. A shore-parallel 455-m-long detached breakwater was placed in $S1$, seaward of the inlet at the 7 m depth contour. For $S2$, a dogleg-jetty was built with a 280-m-long inner segment perpendicular to the shore, and a 265-m-long outer segment extending seaward at a 45° angle toward the inlet. $S3$ was a natural inlet without jetties and with two equal-width barrier islands on each side. Two jetties, each 170 m long, were constructed in $S4$ that were oriented perpendicular to the straight shorelines of the barrier islands [Fig. 2(a)].

The $S1$ and $S2$ inlets were tested for quantifying combined wave diffraction, refraction, and shoaling caused by sloping bottom, jetties and breakwaters. Wave refraction and diffraction were measured in the bay side of $S3$ and $S4$ inlets. Two irregular and one regular wave condition were tested in the experiments for $S1$ – $S4$ inlets. The irregular wave conditions in full-scale represented a short-period wave (mean period of 5.7 sec in prototype), denoted as $X1$, and a long-period wave (mean period of 11.3 sec), denoted as $X2$. The regular wave condition ($X3$) was a short-period wave (5.7 sec in prototype). Ebbing currents were not tested in these

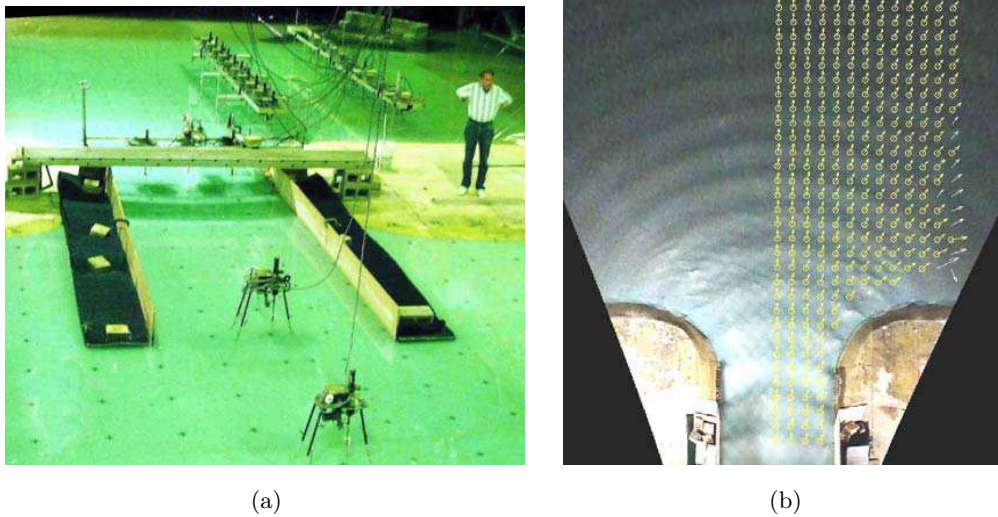


Fig. 2. Experiment *S4* inlet configuration and wave pattern. (a) Configuration for *S4* and (b) wave diffraction into bay for Configuration *S4*.

experiments. A flood current of 1 m/sec (prototype) was used at the throat of *S3* and *S4* inlets to investigate wave-current interaction. Wave diffraction pattern in the bay side of *S4* experiments is depicted in Fig. 2(b).

Twenty wave gauges measured the *in situ* wave heights. The calculated wave heights are compared to measured wave heights from these gauges. Wave directions were obtained by a video camera system as well as a pair of ADVs [Curtis *et al.*, 2001 and 2002; Seabergh *et al.*, 2002]. Wave directions measured by the ADVs were used in checking the accuracy of wave direction from the video-camera system. The differences between two measured spectral peak vector-mean wave directions were quantified by standard deviation and root-mean square error (rmse). For the four configurations investigated, the rmse ranged from 4.6° to 13° . For additional information about Phase I experiments, readers are referred to Seabergh *et al.* [2002] and Lin and Demirbilek [2005] for data collection, analysis, and validation of numerical models.

2.3. Phase II experiments

A second laboratory experiment was designed in 2005 to obtain both current and wave data in the vicinity of an idealized dual-jetty inlet. In these 1:50 Froude scale [Seabergh *et al.*, 2005a; Lin *et al.*, 2006] experiments, the inlets with fully absorbing and reflective jetties are denoted respectively as Configuration *S5* and *S6* in Figs. 3 and 4. Laboratory experiments were performed with three incident regular (monochromatic) wave conditions: a short wave with small wave height (*X6*), a long wave with moderate wave height (*X7*), and a short wave with large wave height (*X8*). These unidirectional incident waves were generated at an angle of 20° from

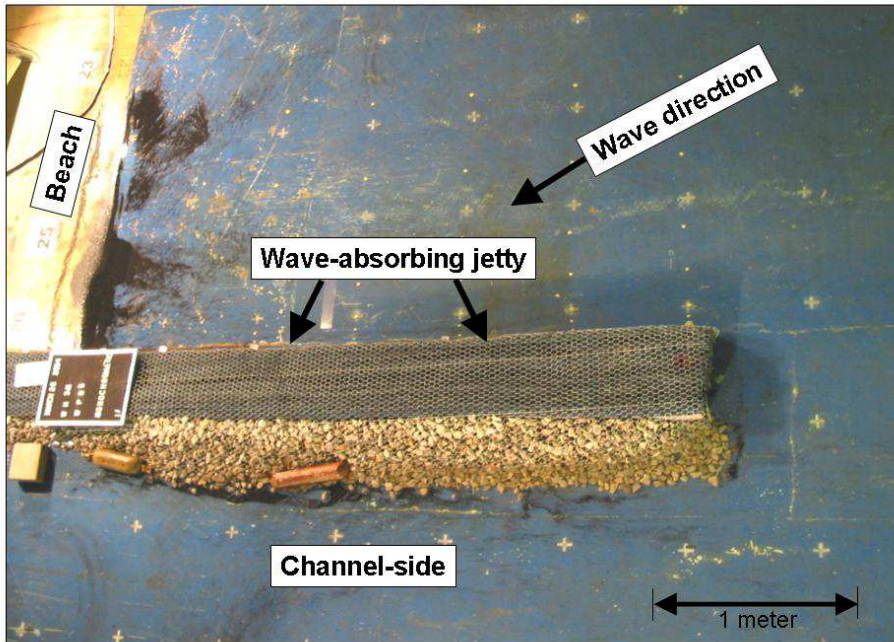


Fig. 3. Photograph of wave-absorbing jetty perpendicular to shore (Configuration *S5*).

the shore normal. The types of monochromatic waves chosen were based on prototype inlet database and wave parameters were selected to ensure wave breaking, and generation of strong current and circulation in inlets and near jetties.

The fully absorbing jetty in *S5* was constructed by lining the up-shore face of a rock jetty with a fibrous material commonly used for wave absorption at the boundaries of physical models (Fig. 3). Wire mesh was used to hold the absorber in place. To maintain the same location of the edge of the jetty as the non-reflecting type, the fully reflecting jetty setup was designed by placing a plywood face (Fig. 4) at the edge of the fibrous material. These experiments were also conducted at a constant still water surface elevation of 1.5 m (full-scale) above the mean low water datum.

For the *S5* and *S6* inlets, waves and currents were measured on the up-wave side of the jetty to the right of inlet. For *S5* inlet, data were also collected inside the inlet between the dual jetties. An array of capacitance wave gauges was used to measure wave height. Currents were measured with ADV instruments, and wave direction was calculated from current vectors data using a stochastic method [Cartwright, 1963]. Details of the Phase II experiments are described in Seabergh *et al.* [2007, 2005a, 2005b].

Sample circulation patterns obtained by injecting dye along the up-wave faces of absorbing and reflecting jetties are shown in Figs. 5 and 6. For the absorbing jetty, a dye patch was initially introduced into the model as shown in Fig. 5 in the

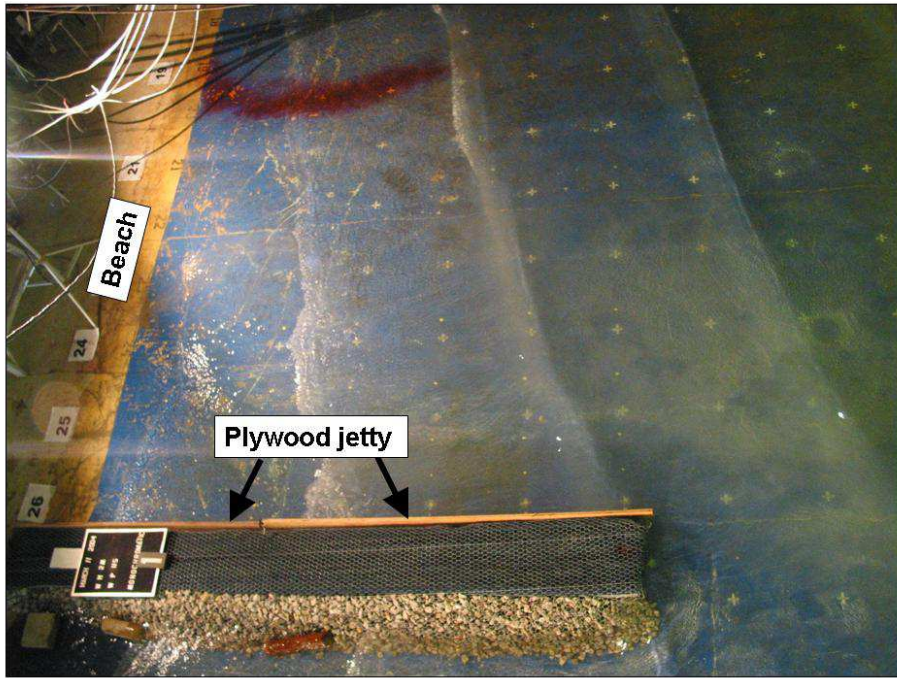


Fig. 4. Photograph of plywood reflecting jetty face (Configuration S6).

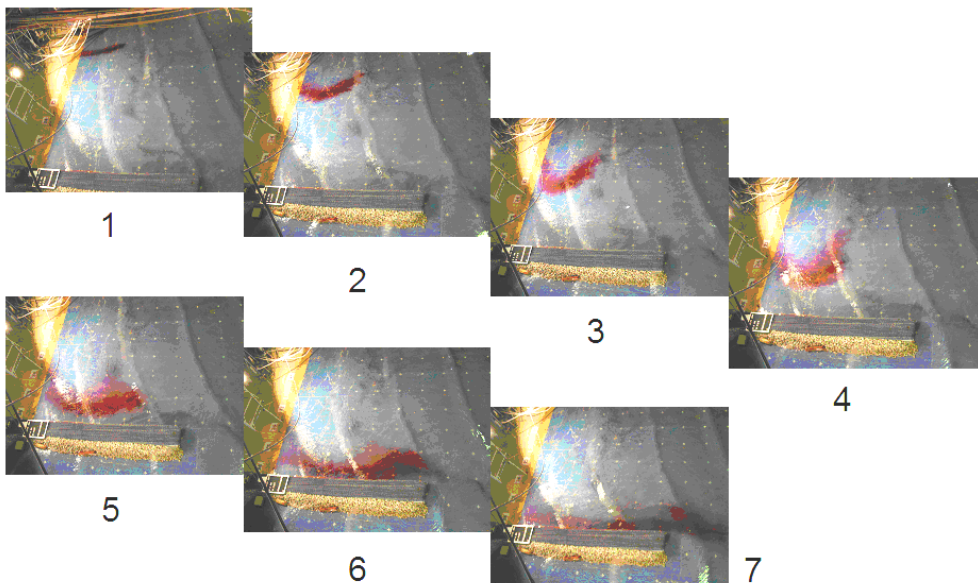


Fig. 5. Sequence of photographs of dye patch approaching the absorbing jetty in Configuration S5 (2-m, 11-sec wave).

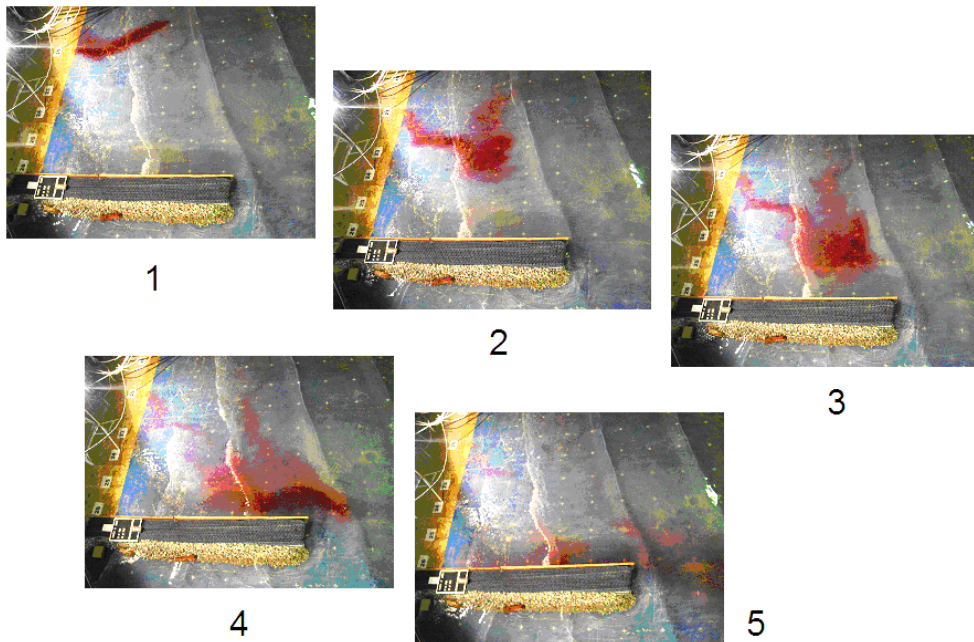


Fig. 6. Sequence of photographs of dye patch approaching the reflecting jetty in Configuration S6 (2-m, 11-sec wave).

first snapshot (#1). The sequential dye movement was recorded with the snapshots (#2) to (#7) taken approximately 8 seconds apart. As shown in Fig. 5, the dye moved towards the jetty and deflected seaward. The breaker location was located roughly along a line passing through the middle of the jetty. For the reflecting jetty shown in Fig. 6, the dye patch began to move seaward in (#2), and further seaward as depicted in frames (#3) to (#5). The waves for the reflecting jetty experiment created a clockwise circulation in the region along the shoreward half of the jetty length. The incoming longshore current was deflected by this circulation seaward further up-drift than for the absorbing jetty experiment. The difference in the near jetty circulation patterns between reflecting and absorbing jetty experiments was clearly evident in the current velocity measurements as well as in the results of numerical model simulations.

3. Numerical Models

The CMS was set up to calculate inlet hydrodynamics near the jetties for comparison with the Phase I and Phase II data sets from physical model studies. As was noted earlier, the CMS-Wave is a 2D nearshore wave spectral transformation model with theoretically sound approximations of wave diffraction [Rivero *et al.*, 1997a, 1997b; Yu *et al.*, 2000; Mase and Kitano, 2000; Mase, 2001; Holthuisen *et al.*, 2004; Mase *et al.*, 2005; Lin and Demirbilek, 2005] and reflection. In addition to linear

wave propagation, dissipation, refraction, and shoaling, wind wave generation was implemented to model complex wave processes at coastal inlets [Lin *et al.*, 2006; Demirbilek *et al.*, 2007; Lin *et al.*, 2008]. The model employs a forward-marching, finite-difference method to solve the wave-action conservation equation [Mase, 2001]. Wave diffraction is implemented by adding a diffraction term to the wave-action-balance equation derived from the parabolic wave equation [Mase *et al.*, 2005]. CMS-Wave operates on a half-plane to allow waves to propagate from the seaward boundary toward shore with forwarding-marching calculations.

The diffraction capability of the CMS-Wave was originally tested for waves in a gap between two breakwaters. Model estimates were compared to the classical analytical Sommerfeld solution of Penney and Price [1952] on a uniform-depth bottom, and for waves transforming over a circular shoal in a laboratory experiment [Mase and Kitano, 2000; Mase, 2001; Mase *et al.*, 2005]. The effect of currents on waves is included as a Doppler shift in the solution of intrinsic frequency calculated through the wave dispersion equation. This type of wave-current interaction has been successfully used in other classes of wave models [Isobe, 1998; Panchang and Demirbilek, 1998; Smith *et al.*, 1999; Lin and Demirbilek, 2005].

CMS-Flow is a time-dependent, 2D rectangular grid circulation and sediment transport model [Buttolph *et al.*, 2006; Camenen and Larson, 2007] that can be forced by tides, waves, surface winds, and flow influx along the computational domain boundary. The wave and flow models were coupled in the present study to calculate wave-current interaction at inlets. Wave radiation stresses from wave model are input to the flow model to calculate wave-induced current [Longuet-Higgins and Stewart, 1964]. The coupling of circulation and wave models is ideal for long-term hydrodynamics and sediment transport simulations when wave fields are updated at a fixed time interval (i.e. hourly or 3 hourly interval). Numerical simulations were performed for the dual-jetty inlet with fully reflecting jetties (*S4* and *S5*) and absorbing jetties (*S6*).

The wave and flow simulations used the same numerical grid. The grid origin is at $x = 450$ m and $y = 300$ m, grid cells are each 10 m by 10 m, and thirteen cells covered the inlet width of 130 m. The dimensions of the numerical grid are 1600 m (or 160 cells) in the cross-shore direction (x -axis) and 1800 m (180 cells) along shore (y -axis), with the inlet located approximately in the grid center. The model domain covered an area of approximately 2 km by 1.5 km, extending 940 m to the left, 730 m to the right of the inlet, 790 m offshore to a depth contour of 15 m, and 570 m bayward of the two barrier islands. A 5 m by 5 m test grid was used to evaluate sensitivity of model results to grid size. This test showed wave model results were not sensitive to grid size, and maximum difference in flow model velocities was less than 10 percent. Because run time increased nearly 4-fold, and the coarser grid was used in the simulations reported here. Input to wave model at the offshore boundary was a JONSWAP-type unidirectional wave spectrum discretized into 30 frequency bins and 35 direction bins, with peak enhancement factor (γ) values of 3.3

and 200 for irregular and monochromatic waves, respectively. In the wave model, a reflection coefficient of 0 or 1 was assigned to the absorbing and reflective jetties, respectively. The shoreline was assigned a reflection coefficient of 0.1. Four incident wave conditions were used in the dual-jetty *S4* inlet simulations, designated here as *X1*, *X2*, *X3*, and *X5*. Incident wave direction was shore normal. Two oblique (20°) regular wave conditions were simulated for *S5* and *S6* configurations.

Two statistical parameters were calculated to evaluate the numerical model performance. The first parameter is defined as

$$E_{\text{rel}} = \frac{1}{N} \sum \left| \frac{R_n - R_e}{R_{\text{ref}}} \right| \quad (1)$$

where E_{rel} is the mean of the absolute relative error between numerical predictions R_n and experimental data R_e , and N is the number of data points. This parameter represents the percent change of model versus measured quantities relative to a reference quantity, R_{ref} . The R_{ref} is either the incident wave height in the wave height error calculation or the maximum measured current speed in the current magnitude error estimate.

The second parameter is the mean of the absolute difference, defined as

$$E_{\text{abs}} = \frac{1}{N} \sum |R_n - R_e| \quad (2)$$

The first parameter is better for comparison of wave height and current magnitude estimates. The second parameter is more suitable for comparison of wave or current directions.

3.1. Comparison of numerical model and Phase I experimental data

Fully reflective jetties made of plywood were used in structural configurations of the Phase I experiments. A detached shore-parallel breakwater (*S1*), a hook-shape breakwater (*S2*), a natural inlet (*S3*), and a dual-jetty inlet (*S4*) were investigated

Table 1. Test conditions for idealized inlet configuration *S4* (1:50 Scale).

Experiment Number	Wave Height (m)	Wave Period (sec)	Wave Direction (deg)	Type	Current on/off
<i>S4</i> : Dual jetties (inlet and bay measurements)					
<i>S4X1</i>	3.05	5.7	0	Irregular	Off
<i>S4X2</i>	2.3	11.3	0	Irregular	Off
<i>S4X3</i>	2.3	5.7	0	Regular	Off
<i>S4X5</i>	2.3	11.3	0	Irregular	Flood

Note: Maximum steady flood current is 1 m/sec at the inlet for *S4X5*. Incident waves are unidirectional and direction is relative to shore-normal.

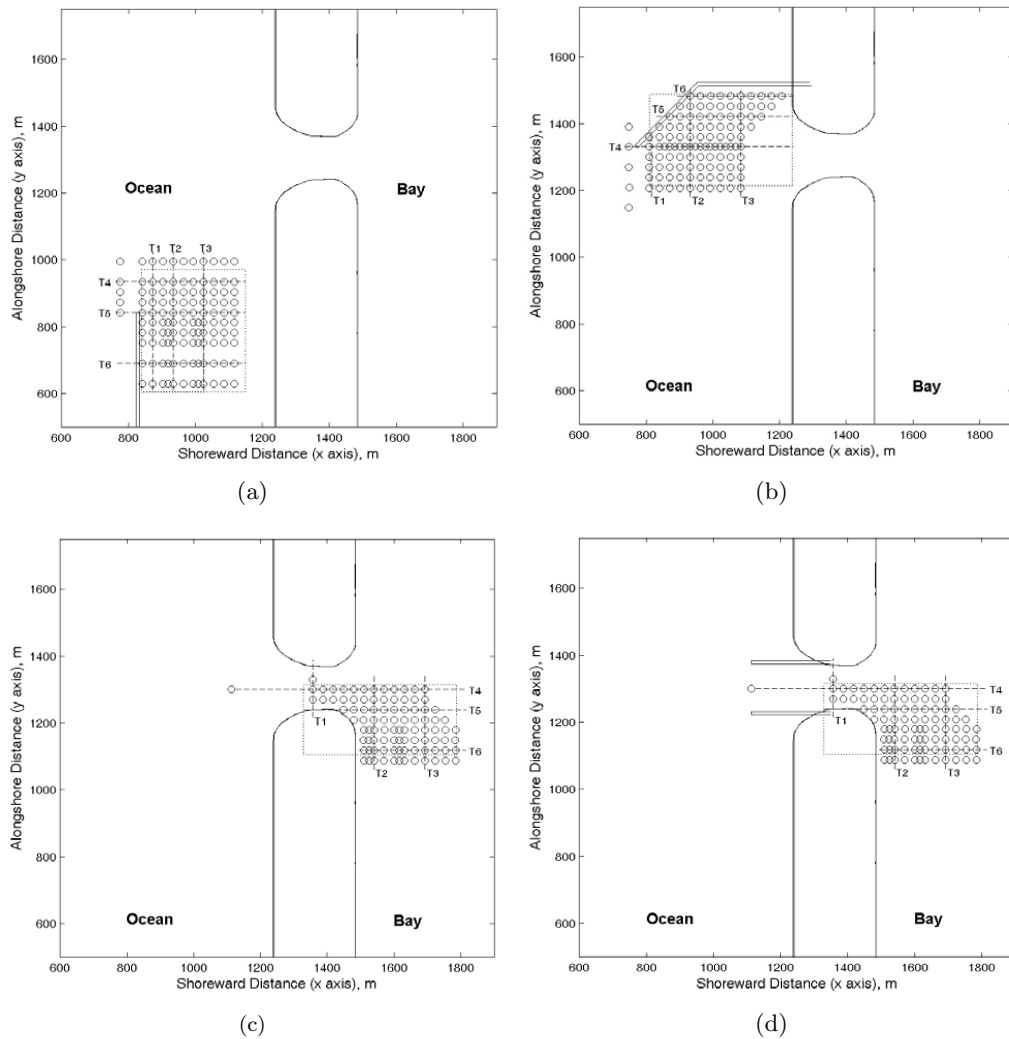


Fig. 7. Location map of wave gauges (circle), the rectangular area covered by the video-camera system (dotted line), and transect lines (dash line) for model and measured wave comparisons in Configurations (a) $S1$, (b) $S2$, (c) $S3$, and (d) $S4$.

(Fig. 7). The numerical model and physical model measurements will be compared only for the dual-jetty inlet configuration ($S4$) for quantifying effects of wave diffraction and reflection at a jettied-inlet. Table 1 provides a list of prototype test conditions (scale 1:50), where incident waves consisted of a regular (monochromatic) wave of period 5.7 sec and two JONSWAP-type irregular (spectral) unidirectional waves with peak periods of 5.7 and 11.3 sec. Incident wave angles were 0° (normal to the shoreline). Froude scaling was applied to achieve prototype conditions for wave height and period and associated wave-induced current. The $S4X5$ test condition had a constant flood current of 1 m/sec at the inlet throat. The wave height measurements had 1 percent error, and wave direction measurements which

were further calibrated with ADVs, had 7.7° error in the *S4* experiments. As shown in Fig. 7 (scaled 1:50 to prototype), wave data in these experiments were collected between jetties and in the backbay [Seabergh *et al.*, 2002; Lin and Demirbilek, 2005].

Three types of numerical wave simulations were performed for each physical model test condition:

- (a) wave alone simulation for the non-reflecting (fully absorbing) jetty with a zero reflection coefficient R in the model,
- (b) wave simulation for the fully reflecting jetty ($R = 1$) configuration, and
- (c) coupled wave and flow simulation with $R = 1$ for wave-current interaction.

The same grid was used in both wave and circulation models. For coupled wave and flow, the wave field was calculated initially without the current field and updated at 3-hr interval after the current field was calculated between two consecutive wave field estimates. A hydrodynamic time step of 1 sec is used in the circulation model to satisfy the Courant criterion for stable numerical solutions. Calculated results were not sensitive to the hydrodynamic time step. Wave radiation stresses computed by the wave model are used in the flow model in a 6-hr simulation performed with the coupled models. The run-time for a 6-hr simulation with time step of 1 sec was approximately 4.5 hr on a 2-GHz PC. For the *S4X5* experiment, a flood current was simulated in the circulation model by specifying the water level gradient between the seaward and bay-ward boundaries of flow model.

In the *S4* inlet simulations, calculated wave heights were compared to measurements along six transects (Fig. 7) inside the inlet (navigation channel) and also in the diffracted wave area in the back-bay. All numerical simulations and comparison to measurements were conducted at the prototype scale. Figure 8 shows comparison of calculated wave height and direction with data along six transects for *S4X1* corresponding to a fully reflecting jetty ($R = 1$) and coupled wave-circulation models. The largest differences between the calculated results and data occurred for wave directions. For wave heights, differences between calculated results and data were comparatively less, and limited to areas where wave heights were small. Calculated wave heights and directions are compared with data in Fig. 9 for *S4X3* with absorbing ($R = 0$) and fully reflecting ($R = 1$) jetties. Figure 10 shows comparison for *S4X5* corresponding to the reflecting jetty ($R = 1$) and coupled wave-circulation models. These figures show that calculated wave heights generally follow data at the inlet (Transect 1), and agreement improving for the coupled simulation as compared to wave model alone simulation. This model-data agreement at the inlet further assures the reliability of wave estimates in the backbay area.

Three statistics were used to express the level of agreement between the calculated wave results and the measurements. The first statistic is the mean of the absolute relative error of wave height, [Eq. (1)], representing the percent change of calculated wave height and data. The second is the mean of the absolute difference

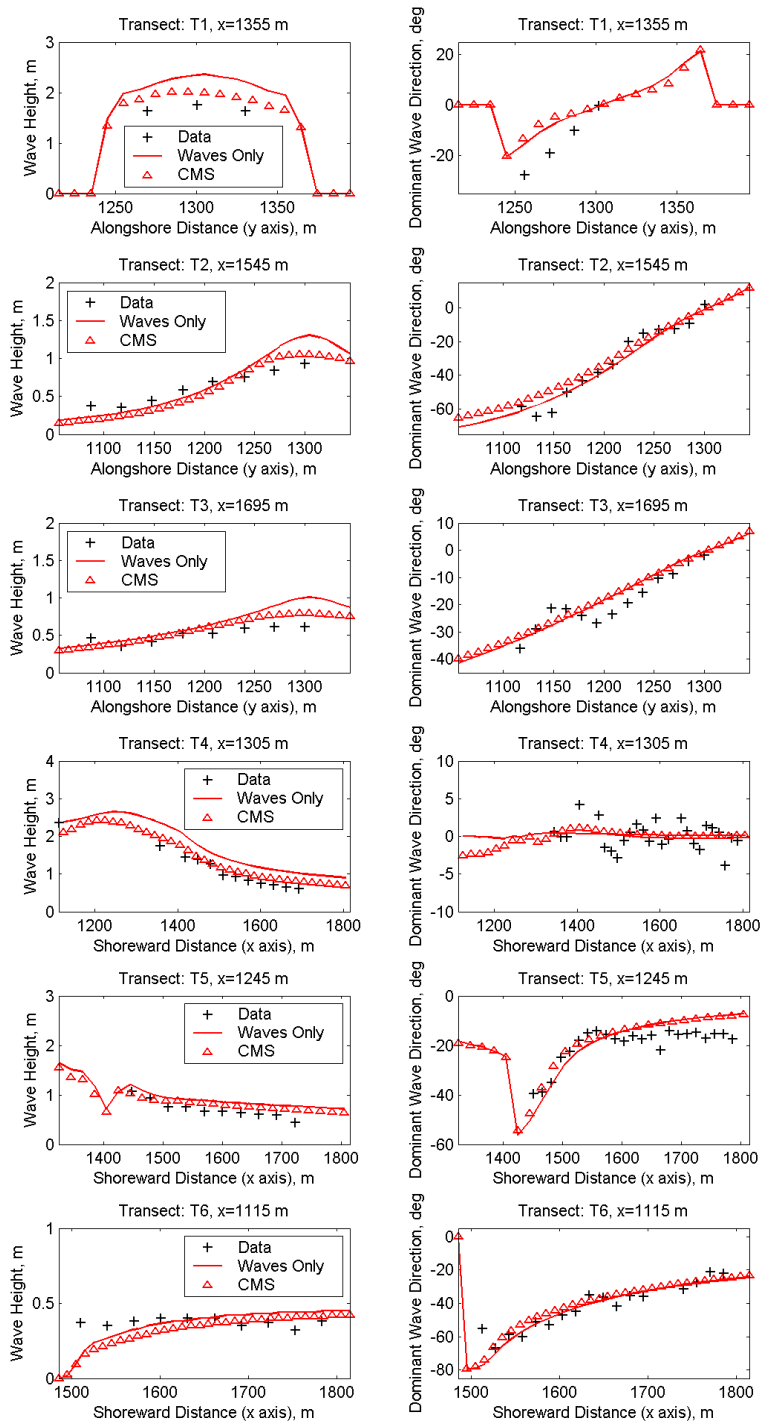


Fig. 8. Calculated versus measured wave height and direction for $S4X1$ ($R = 1$).

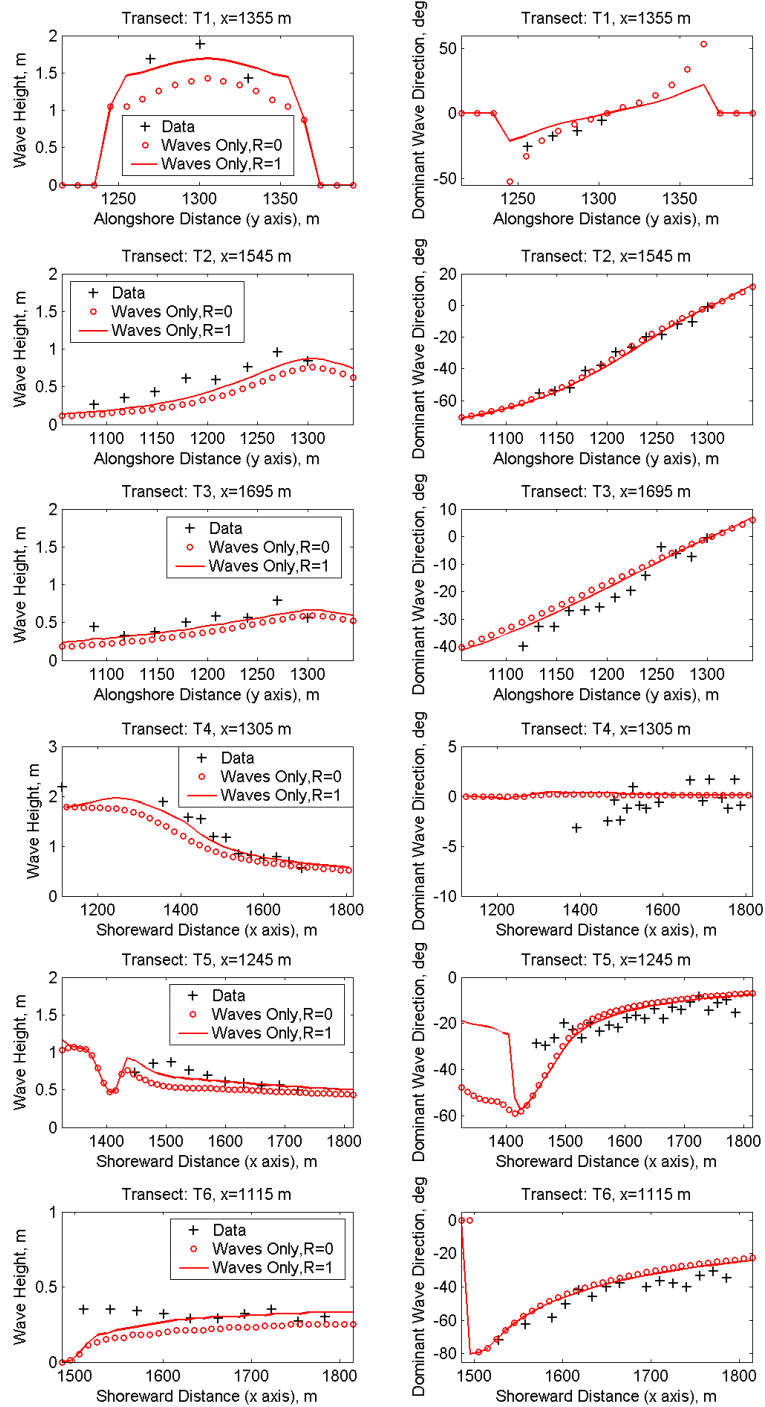


Fig. 9. Calculated versus measured wave height and direction for S4X3 ($R = 0$ & $R = 1$).

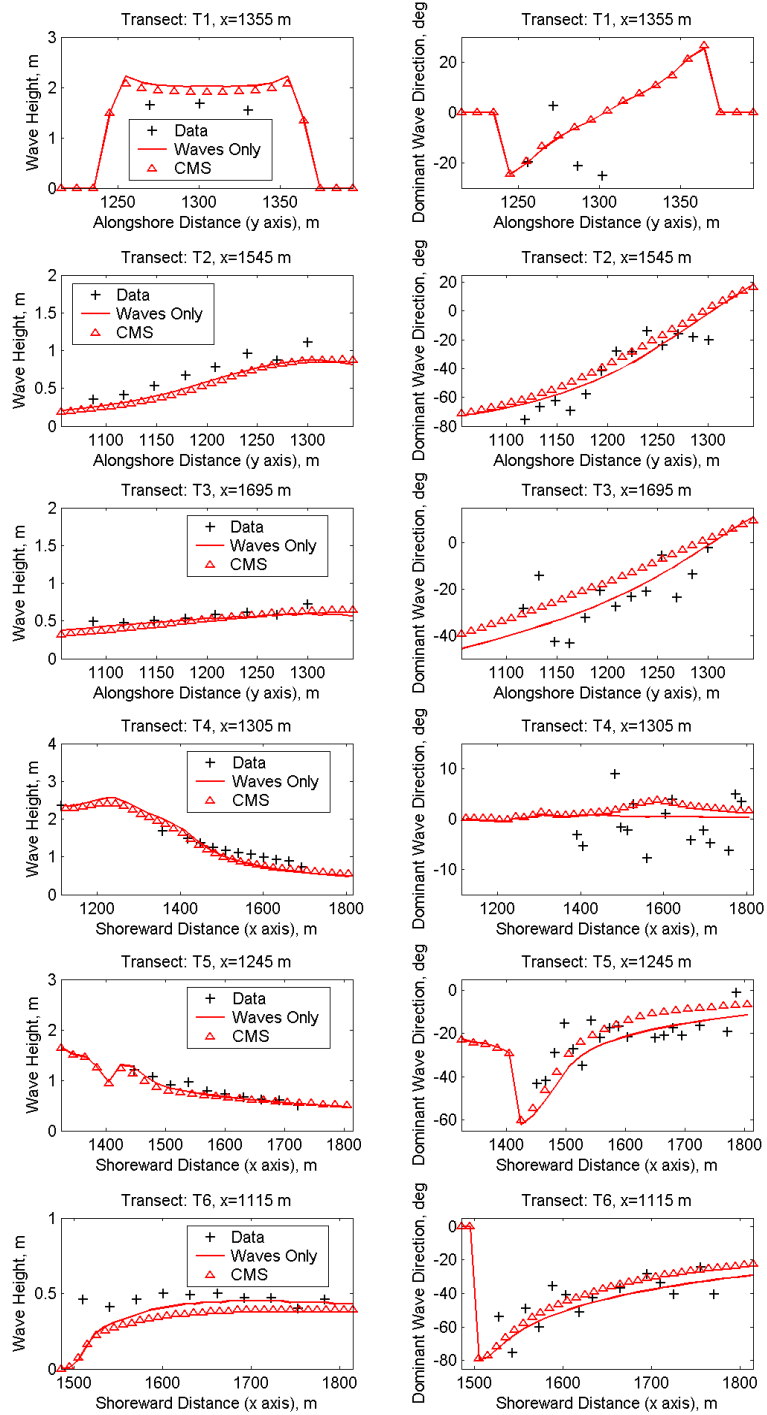


Fig. 10. Calculated versus measured wave height and direction for $S4X5$ ($R = 1$).

Table 2. Statistical errors of calculated height and direction for *S4*.

Experiment Number	Mean of Absolute Relative Wave Height Error (%)*	Mean of Absolute Wave Height Error (m)	Mean of Absolute Wave Direction Error (deg)
Simulation with $R = 0$ for jetties			
<i>S4X1</i>	4.9	0.15	3.6
<i>S4X2</i>	8.7	0.20	7.6
<i>S4X3</i>	8.3	0.19	4.7
<i>S4X5</i>	13.5	0.31	7.8
Average	8.9	0.21	5.9
Simulation with $R = 1$ for jetties			
<i>S4X1</i>	7.5	0.23	3.6
<i>S4X2</i>	6.1	0.14	7.8
<i>S4X3</i>	3.1	0.07	4.3
<i>S4X5</i>	5.7	0.13	7.6
Average	5.6	0.14	5.8
Simulation with $R = 1$ and coupling with CMS-Flow			
<i>S4X1</i>	4.3	0.13	3.7
<i>S4X2</i>	6.1	0.14	7.5
<i>S4X3</i>	7.0	0.16	4.9
<i>S4X5</i>	6.1	0.14	8.4
Average	5.9	0.14	6.1

Note: Waves were updated on a 3-hr interval in the coupled CMS-Flow and CMS-Wave simulations and duration of each simulation was 6 hr.

*The error estimate is relative to the incident wave height.

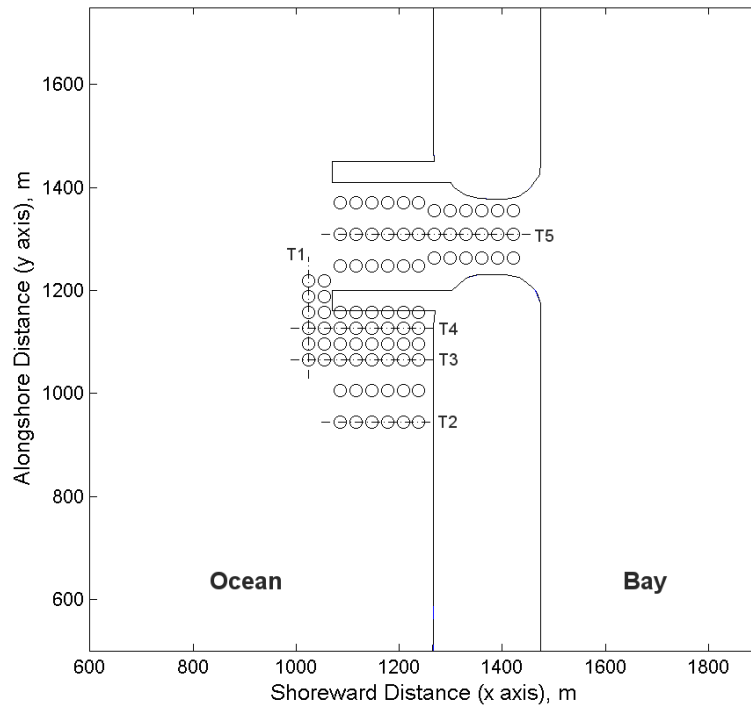
(bias) for wave height, [Eq. (2)]. The third is the mean of the absolute difference of calculated and measured wave directions [Lin and Demirbilek, 2005]. Wave period is not considered in the comparison because it did not change in the physical and numerical models. Table 2 presents a comparison of the three mean statistics for each of the test condition as averaged over each alongshore and cross-shore transect. The difference between different numerical simulation results ($R = 0$, $R = 1$ for wave, and $R = 1$ for coupled wave and flow) is notable. These statistics indicate the wave model predicts reliable wave height estimates with $R = 1$ for a fully reflecting jetty. Wave direction estimates obtained for the shorter irregular wave (*S4X1*) have the smallest mean error of 3.6° for $R = 0$ and $R = 1$. The corresponding error for the coupled simulation of wave and flow is 3.7° . Values of calculated wave direction errors are similar for all *S4* experiments.

3.2. Comparison of numerical model and Phase II experimental data

A fully absorbing jetty inlet (*S5*) and a fully reflecting jetty inlet (*S6*) were tested in the Phase II experiments. These experiments did not include a flood or ebb current at the inlet. Numerical simulations were conducted only for the moderately long

Table 3. Fully absorbing and reflecting jetty experimental condition (1:50 scale).

Experiment Number	Wave Height (m)	Wave Period (sec)	Wave Direction (deg)	Type	Current on/off
Fully absorbing jetty, <i>S5</i>					
<i>S5X7</i>	2.0	11	-20	Regular	Off
<i>S5X8</i>	3.4	8	-20	Regular	Off
Fully reflecting jetty, <i>S6</i>					
<i>S6X7</i>	2.0	11	-20	Regular	Off
<i>S6X8</i>	3.4	8	-20	Regular	Off


 Fig. 11. Location map of current and wave measurement stations (circle) and transect lines (dashed line) for wave model and data comparisons — Configurations *S5* and *S6*.

wave (*X7*) and for the steep, large short wave (*X8*). Table 3 lists the incident wave conditions (scaled by 1:50 to a prototype dimension). Both waves and wave-induced currents were measured in the physical model. Numerical model results were compared to data at the current and wave measurement stations (Fig. 11).

For *S5*, numerical simulations were made with wave alone and coupled flow and wave with $R = 0$ specified in the wave model for the fully absorbing jetty.

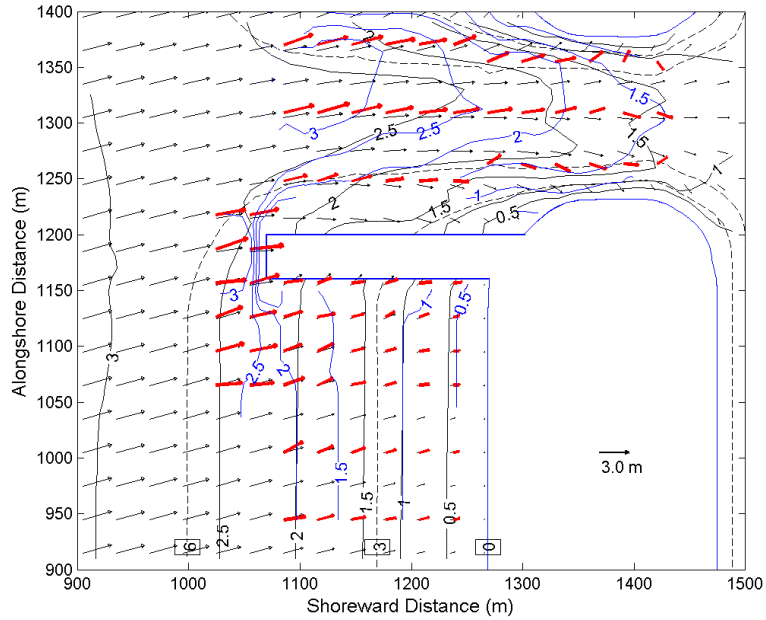


Fig. 12. Calculated versus measured wave fields for S5X8 (measured wave shown in dark vectors; wave height in solid contours; and depth contours by dash lines).

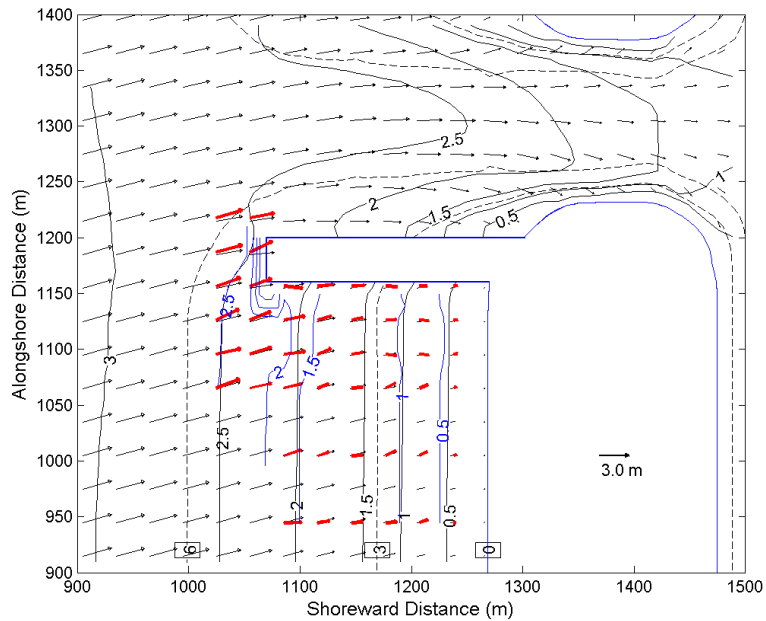


Fig. 13. Calculated versus measured wave fields for S6X8 (measured current shown in dark vectors; wave height in solid contours; and depth contours by dash lines).

Coupling between wave and flow models was at a 3-hr interval and the duration of simulation was 6 hr. In the coupled simulations for *S6*, $R = 1$ was specified in the wave model to represent a fully reflecting jetty. To illustrate, Figs. 12 and 13 show the calculated and measured wave fields in full-scale for test conditions *S5X8* and *S6X8*, respectively. In these figures, calculated wave height and direction are shown as black vector quantities and wave height is shown in black contours. Measured wave height and direction data are depicted in red vectors and blue contours. For the absorbing jetty, the best agreement between model and data is obtained inside the inlet channel. At the up-wave side of the jetty inlet, model and data compare favorably near the shore, but significant differences between wave-height contours appear starting halfway along jetty. The largest difference occurs for the reflecting jetty for the incident long wave condition *S6X7*.

Figures 14 and 15 show a sample comparison of calculated and measured wave heights and directions for *S5X8* and *S6X8*, respectively, along transects *T1–T5*, located south of the up-wave jetty and inside the inlet area (see Fig. 11). Table 4 presents the calculated mean statistical errors, relative and absolute, between numerical estimates and measurements for *S5X7*, *S5X8*, *S6X7*, and *S6X8* along five transects. These errors for wave height and direction were calculated for wave-only and coupled simulations. Both the wave-alone and coupled wave and flow simulations reproduced the wave fields in the inlet area for both absorbing and fully reflecting jetties. The coupled wave and flow simulations captured overall features of the circulation field induced by incident waves, with notable differences in the number, size, and shape of the calculated vs observed circulation cells. This means

Table 4. Statistical errors of calculated wave height and direction for *S5* and *S6*.

Experiment Number	Mean of Absolute Relative Wave Height Error (%)*	Mean of Absolute Wave Height Error (m)	Mean of Absolute Wave Direction Error (deg)
Simulation by CMS-Wave			
<i>S5X7</i>	15.0	0.30	7.6
<i>S5X8</i>	8.9	0.30	5.9
<i>S6X7</i>	12.5	0.25	9.5
<i>S6X8</i>	5.6	0.19	7.2
Average	10.5	0.26	7.6
Simulation by CMS-Flow and CMS-Wave			
<i>S5X7</i>	12.0	0.24	7.0
<i>S5X8</i>	7.4	0.25	6.9
<i>S6X7</i>	14.0	0.28	9.0
<i>S6X8</i>	6.5	0.22	7.5
Average	10.0	0.25	7.6

Note: Waves were updated on a 3-hr interval in the coupled CMS-Flow and CMS-Wave simulations and duration of each simulation was 6 hr.

*The error estimate is relative to the incident wave height.

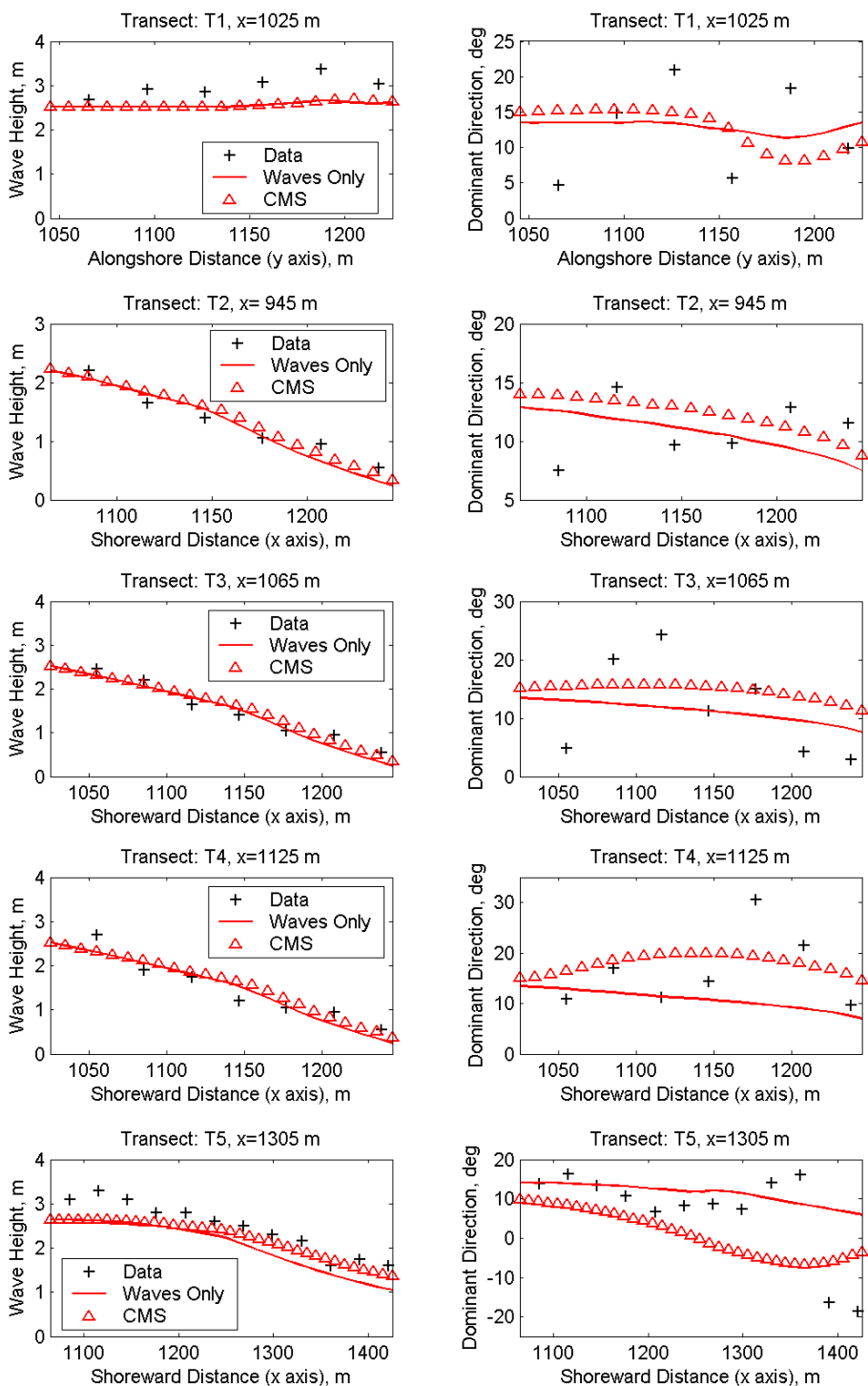


Fig. 14. Calculated versus measured wave height and direction for S5X8.

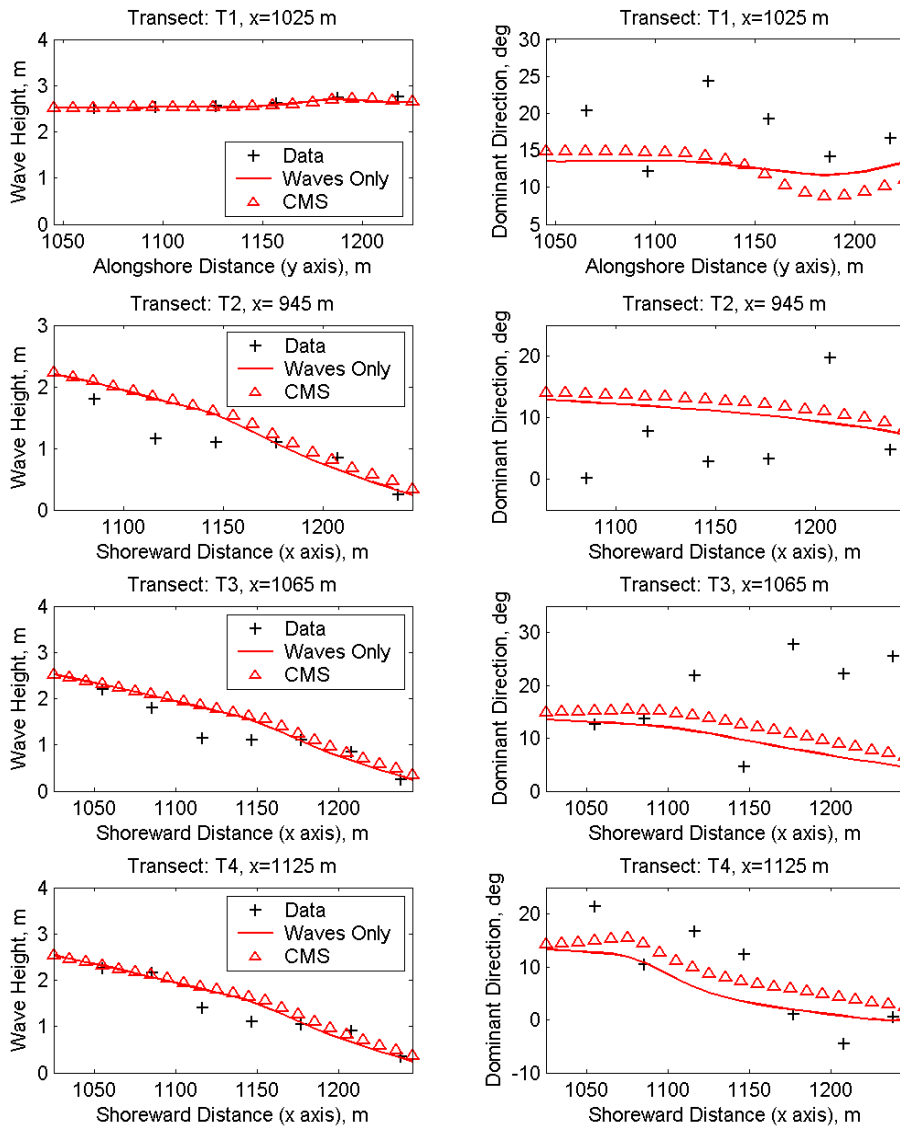


Fig. 15. Calculated versus measured wave height and directions for *S6X8*.

that un-calibrated numerical models can provide useful insight to inlet hydrodynamic processes, but may not adequately resolve finer details of flow near inlet structures as induced by sub-wavelength wave processes such as wave breaking, turbulence, reflection and diffraction. 3D flow models or 2D Boussinesq-type circulation models with turbulence modeling capability [Nwogu and Demirbilek, 2001] may be necessary to properly resolve complex flows that develop near jetties.

Examples of calculated wave-induced current fields (black vector) and measured currents (red vector) for *S5X8* and *S6X8* are shown in Figs. 16 and 17. For the

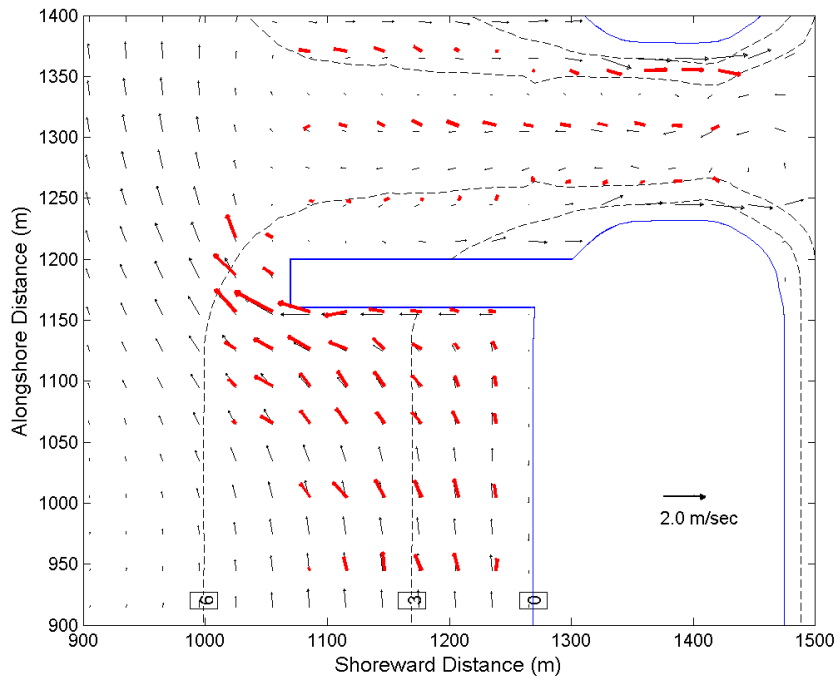


Fig. 16. Calculated versus measured current fields for *S5X8* (measured current shown in vectors; depth contours indicated by dash lines).

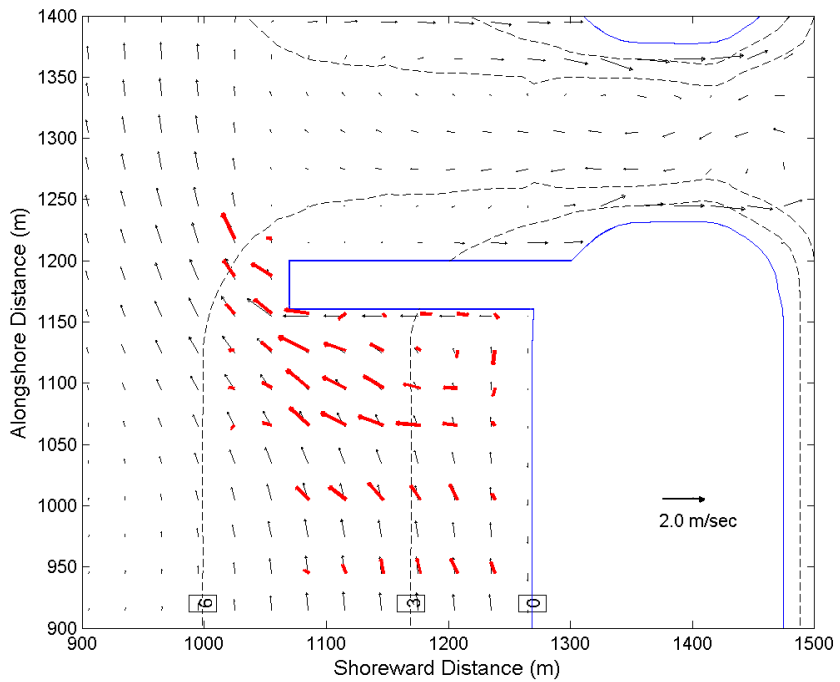


Fig. 17. Calculated versus measured current fields for *S6X8* (measured current shown in vectors; depth contours indicated by dash lines).

Table 5. Statistical errors of calculated current speed and direction for *S5* and *S6*.

Experiment Number	Mean of Absolute Relative Current Speed Error (%) [*]	Mean of Absolute Current Speed Error (m/sec) ^{**}	Mean of Absolute Current Direction Error (deg)
Simulation by CMS-Flow and CMS-Wave			
<i>S5X7</i>	16.1	0.31 (1.93)	27.8
<i>S5X8</i>	11.6	0.26 (2.24)	21.9
<i>S6X7</i>	25.6	0.42 (1.64)	40.5
<i>S6X8</i>	26.5	0.45 (1.70)	43.3
Average	20.0	0.36 (1.88)	33.4

Note: For coupling CMS-Flow and CMS-Wave, the two models were run alternatively in the 3-hr interval for a total of 6-hr simulation.

^{*}The error estimate is relative to maximum measured current speed.

^{**}Maximum measured current magnitude is shown in parentheses.

absorbing jetty case, the trend of the calculated current agrees with the data at the up-wave side of jetty (south) and inlet area. However, the coupled wave and flow simulation was unable to reproduce the circulation cells that developed at the up-wave area of the reflecting jetty which were observed in the laboratory experiments. This discrepancy may be attributed to:

- (1) weak reflection and diffraction estimates by the wave model in the areas adjacent to structures,
- (2) errors in the calculated wave radiation stress gradients,
- (3) methods used for wave-structure interaction in the flow model, and
- (4) potential 3D flow effects that the 2D flow model is not expected to represent.

Along the centerline of the inlet channel, the coupled models predicted a return current flowing from bay to ocean as was observed in the physical model tests. Calculated current speed and direction versus data along transects of *S5* and *S6* for the incident wave condition *X8* are shown in Figs. 18 and 19. These figures show that the coupled models predicted currents better for an absorbing jetty than for a reflecting jetty. The circulation cells observed at the up-wave side of the reflecting jetty in the laboratory could not be reproduced by the coupled models. Calculated mean statistical errors by Eqs. (1) and (2) are provided in Table 5 for the calculated current speed (maximum error 20 percent) and direction (maximum error 33.4°) along transects *T1–T5* located in the up-wave jetty (south) and inside the inlet. The error estimate calculated by Eq. (1) is relative to maximum measured current speed, a representative current used for scaling current speeds. Other current speeds, such as the maximum current speed at the inlet throat or the largest current within the inlet, could also have been used.

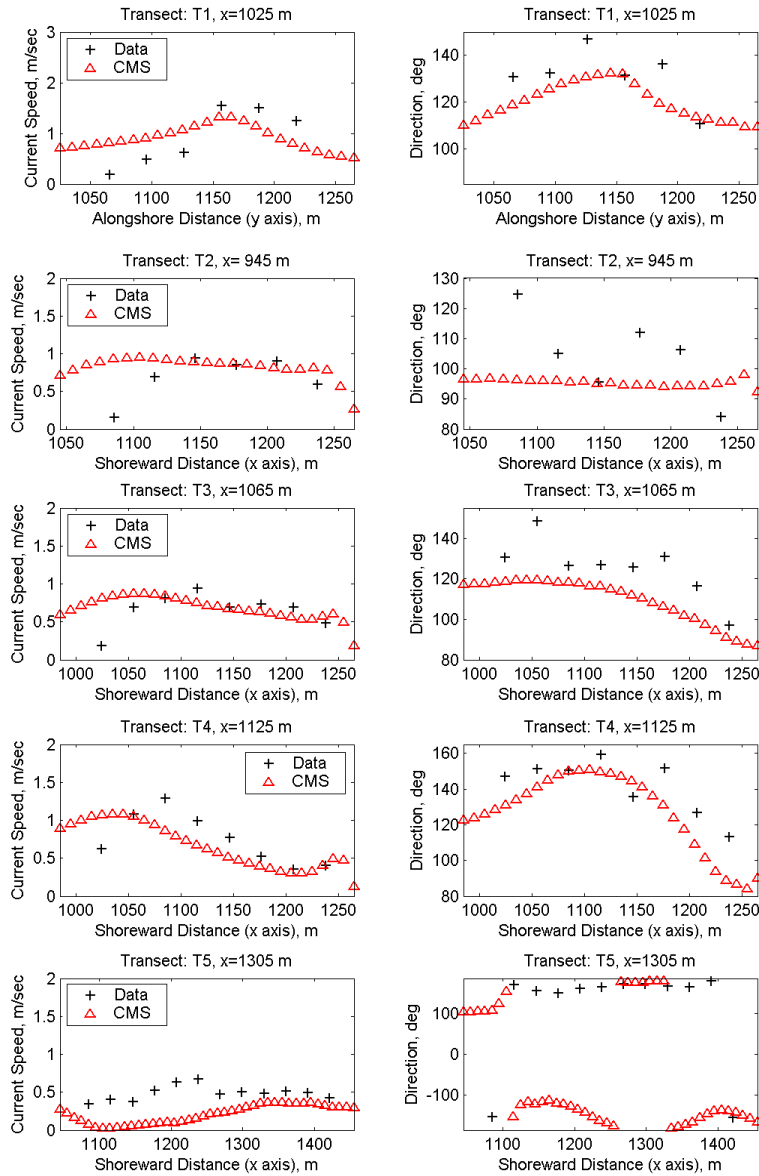


Fig. 18. Calculated versus measured current speed and direction for S5X8.

4. Discussion of Numerical Model Performance

The laboratory data used in the present study covers a wide range of conditions for coastal inlets with and without jetties, inlets with absorbing and reflective jetties, and a variety of incident wave combinations including swell and local wind-waves of different height, period, and direction. This diversity provided an excellent opportunity to investigate the capability of numerical models for a range of incident wave conditions and different inlet configurations. The following observations were

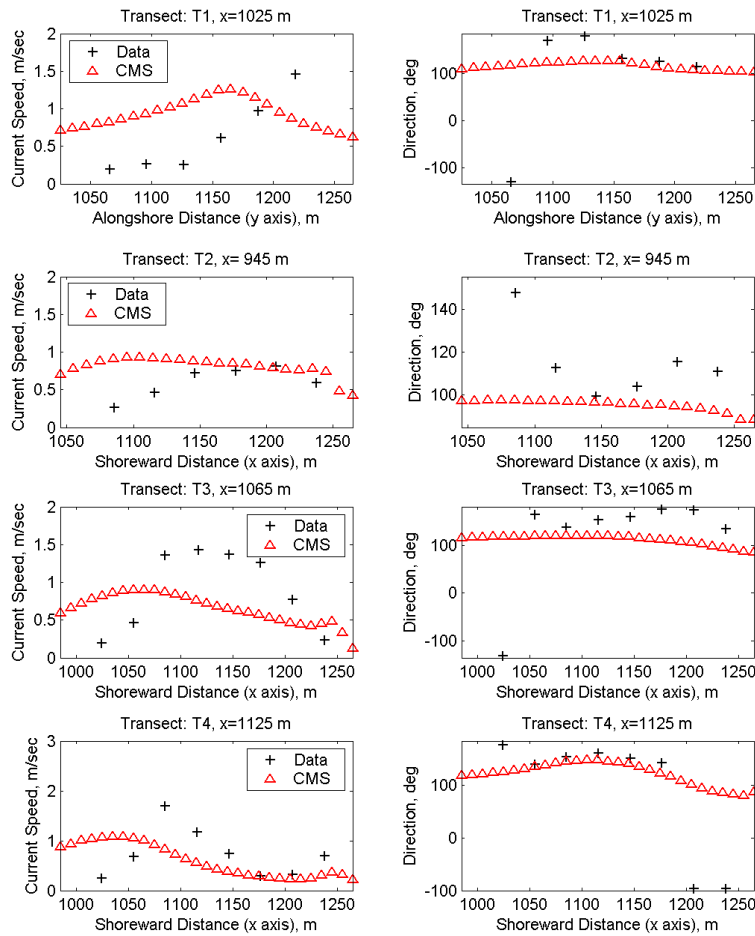


Fig. 19. Calculated versus measured current speed and direction for S6X8.

made by comparing model results and data for different type of inlets through a series of numerical sensitivity simulations conducted for improving models performance.

Notable differences in the hydrodynamic characteristics were observed in the physical model studies for two extreme jetty structures: reflective versus absorbing jetties. For the absorbing jetty, waves generally broke at the jetty with no visible evidence of reflection. Located on the up-wave side of inlet, this jetty deflected the longshore current, turning it seaward nearly 90° , along the structure. With a reflective jetty in laboratory experiments, a landward circulation cell was developed, starting about at the mid-section of the jetty and extending all the way to the shoreline. Additional smaller cells developed after the advection and disintegration of the major cell. The main cell was large and strong enough to deflect the offshore movement of littoral currents approximately a distance of one wavelength up the coast.

Numerical models used in this study were able to mimic these general flow patterns, but the models could not replicate the detailed circulation pattern associated with each jetty type. Specifically, the circulation cells that developed closest to the jetties and near the ends of structures could not be reproduced. Possible causes of this difference were discussed earlier. The near-jetty circulation varied strongly with the gradients of wave radiation stress developing near the jetty and shore faces. In addition, the cross-shore extent of the longshore current calculated by the numerical models was much wider than what was observed in the experiments. The surf zone current magnitude and circulation in the numerical simulations were sensitive to grid resolution, time step, bottom friction, and eddy viscosity coefficients. Another factor controlling the surf zone dynamics was the interval of wave input used for updating wave-current interaction processes in the circulation model. Shorter intervals for feedback between wave and flow models generally produced slightly better and more stable results.

These differences between model prediction and measurements were attributed to the complexity of modeling wave and flow fields very close to inlet structures. Simulations showed strong gradients occurring in wave height and direction estimates near structures. Numerical approximations involved in the calculation of wave diffraction and reflection at inlet structures may partly explain these differences. Sensitivity tests performed showed that modeling estimates from coupled simulations varied with bottom friction and eddy viscosity coefficients in the flow model. CIRP is presently conducting additional laboratory tests to determine the role of these coefficients.

Three statistics are calculated using Eqs. (1) and (2) for each numerical simulation to compare model performance to data. For *S4*, the mean of absolute relative error is calculated for wave height, and the mean of absolute difference is calculated both for wave height and wave direction. The statistical comparison of waves indicates that calculated wave heights are close to measurements in the inlet channel and bay. The results of wave alone simulations tend to over-predict wave heights for irregular waves (*X1*) and underestimate wave height for regular waves (*X3*). The model predicted the trend of wave direction correctly, but measurements indicated stronger wave diffraction in the backbay area than the model with and without a flood current. This is evident in Figs. 8 and 9 in the diffraction zone for transects *T2* and *T6*.

For *S4*, the fully reflective jetty, the wave model performed better with the reflection coefficient $R = 1$, both for wave alone and coupled simulations, as compared to $R = 0$ (Table 2). Larger errors produced in wave height estimate using $R = 0$ is not representative for the fully reflective jetty tested in the experiment. The overall mean of absolute relative wave height errors for all incident wave conditions is approximately 6 percent for $R = 1$ and 9 percent for $R = 0$. Errors in the wave direction estimate range between 3.6° and 8.4° , respectively, for $R = 0$ and $R = 1$. Smaller errors in wave direction estimate occurred for shorter period wave simulations (*X1*

and $X3$). However, the statistics of wave direction are less reliable in these cases because the relatively large instrumental error (7.7°) is nearly equal or greater than the error in calculated wave direction.

In the case of dual-jetty inlet configuration with a flood current ($S4X5$), the wave model alone and coupled models results were similar for the fully reflective jetty. Small statistical errors in wave height and direction estimates are similar for $S4X5$ simulations with the fully reflective jetty. It has been reported by Holthuijsen *et al.* [2004], and Lin and Demirbilek [2005] that this class of spectral wave models tends to excessively dissipate wave energy due to breaking and wave-current interaction inside the inlet. Such excessive reduction of energy is most likely caused by the type of wave-breaking criteria implemented in wave models. More laboratory and field studies are needed to evaluate the appropriateness of depth-limited wave breaking formulas commonly used in this class of wave models.

For the fully absorbing jetty experiment of $S5$ and fully reflecting jetty of $S6$, similar numerical simulations were performed with wave model alone and also with the coupled wave and circulation models. Incident wave conditions were a regular long wave with moderate wave height ($X7$), and a regular short wave with large wave height ($X8$). Both incident waves were 20° oblique to the shore-normal direction. These experiments were designed for the investigation of wave behavior in the ocean side and between jetties of an idealized inlet. Neither the flood nor ebb current was included in these experiments. The wave-induced current and wave-current interactions were only calculated with coupled models. Numerical grids for wave and circulation models were identical to those used in the $S4$ configuration. The model results were compared to data along that transects both normal and parallel to shoreline inside the inlet and in the up-wave jetty area. Both the mean of absolute relative error and the mean absolute difference were calculated for wave height, wave direction, and current speed.

The comparative statistics of calculated wave heights and directions for $S5$ and $S6$ simulations are similar for fully absorbing and reflective jetties (Table 4). The errors in wave height and direction estimates are also similar for wave-only and for the coupled models. Larger absolute relative wave height error and absolute direction error are obtained for the moderate wave height ($X7$) compared to the large (and steep) wave height ($X8$) test condition.

The error statistics for $S5$ and $S6$ inlets (Table 5) are larger for the magnitude and direction of currents than for wave height. These larger errors are a consequence of the models predicting a wider cross-shore distribution of the calculated longshore current than was measured in the laboratory. Comparatively larger errors occur for current magnitude and direction of the reflecting versus absorbing jetties. These errors may be due to an up-wave jetty side circulation cell observed in the physical model which was not reproduced in the numerical simulations (see Fig. 17). It is certainly possible that the missing gyre in the numerical simulations could be a scale effect or an inherent limitation of the flow model. The mean absolute difference

between the calculated and measured current magnitude for the absorbing jetty is 0.28 m/sec. In contrast, this error is 0.43 m/sec for the reflective jetty. The errors in current direction are approximately 25° and 42° for absorbing and reflecting jetties, respectively. The potential causes of differences in the near structure hydrodynamics for absorbing and reflective jetties, with a particular attention on properly simulating the development of an up-wave side eddy cell, are the subject of ongoing investigations.

The physical model produced a non-uniform wave height distribution of waves entering and exiting the inlet due to combined wave shoaling, reflection, refraction, and diffraction. The wave model was able to capture most of these processes in the wave-only simulations for both absorbing and reflecting jetties. However, strong wave-current interaction plays an important role here, contributing to the differences seen between models and data. In the field, tidal currents and wave-induced currents combined are expected to have even a stronger effect on the dynamics of inlets. Therefore, the coupled models need to be able to handle the strong wave-current interactions that exist in prototype environments. Implementation of wind forcing, wave breaking and dissipation formulas in the wave model are presently in progress. Collectively, these added capabilities should improve the model's performance under such conditions.

5. Conclusions

The objective of the research studies described in this paper was a systematic evaluation of predictive numerical models for inlets, with a special focus on the models' performance in close proximity to inlet structures (i.e. jetties or breakwaters), and their ability to describe the complex flows that exist in inlets and connecting back bays. A spectral wave model and a 2D circulation model were coupled to model inlet hydrodynamics. The coupled modeling system has been tested using extensive datasets obtained from four idealized inlet laboratory experiments conducted for different incident wave conditions and for two types of jetty structures, absorbing and reflective jetties.

In this paper, the performance of CMS-Wave, a new spectral wave transformation model, and its operation within the framework of the CMS for coastal inlet applications is described. Results are provided to calculate wave-induced currents and wave diffraction and reflection from coupling wave and circulation models at coastal inlets. Different types of simulations were performed and the results indicate that wave breaking, diffraction and reflection processes dominate wave transformation at coastal inlets, in particular, those stabilized with jetties. The model results are presented and evaluated in this paper using two laboratory datasets that collected extensive current and wave measurements for four inlet geometries. In general, model predictions follow closely the trends of data for a wide range of current and wave conditions studied in laboratory experiments. Results show the wave model

is capable of describing the effects of wave diffraction and reflection around both absorbing and reflective jetties. Its performance very near the jetties would require further testing with both laboratory and field data.

Calculated current and wave fields at inlets obtained from the coupled wave and flow models are compared to data. Comparison is performed both for regular and irregular incident waves of short and long periods. The coupled modeling system was unable to replicate circulation cells that developed near the end of the reflective jetty. In these simulations, the maximum errors between numerical model predictions and data in wave height and wave direction were 0.4 m and 8.4° , respectively. The wave and circulation models are presently being evaluated in field studies to assess their limitations for practical applications. Numerical tests are in progress for a grid-nesting feature for the wave model to facilitate regional-scale applications. The newly added wave-generation-growth capability of wave model for varying fetch distances and wind speeds is also being tested against field data.

The emphasis of the research presented in this paper is to evaluate the CMS as a coastal inlet predictive tool to demonstrate its suitability for practical applications. The order of errors seen in the wave height and direction estimates suggests that more laboratory and field data are necessary for jettied inlets. This would allow improvement of features of the coupled modeling system for generalized inlet applications and challenging prototype environments. Additional data for different structures and inlets could be used in the calibration of model parameters and to guide users in applying the CMS to real world inlets. Calibration parameters obtained for each evaluation examples and testing conditions, and lessons learned in this research are presently being used by CIRP in the application of CMS to storm-damage assessment, modification to jetties including jetty extensions, jetty rehabilitation and breaching [Demirbilek *et al.*, 2008], addition of spurs to inlet jetties [Seabergh *et al.*, 2007], and barrier islands to protect beaches and improve navigation safety [Lin *et al.*, 2006 and 2008].

Acknowledgments

We extend our appreciation to Dr. Nicholas C. Kraus, the Program Manager of CIRP, for his support and interest in this research. Permission to publish this paper has been granted by the Chief, U.S. Army Corps of Engineers.

References

- Buttolph, A. M., Reed, C., Kraus, N. C., Ono, N., Larson, M., Camenen, B., Hanson, H., Wamsley, T. & Zundel, A. K. [2006] "Two-dimensional depth-averaged circulation model CMS-M2D: Version 3.0, Report 2, sediment transport and morphology change," Coastal and Hydraulics Laboratory Technical Report ERDC/CHL TR-06-9, U.S. Army Engineer Research and Development Center, Vicksburg, MS.
- Cartwright, D. E. [1963] "The use of directional spectra in studying output of a wave recorder on a moving ship," in *Ocean Wave Spectra: Proceedings of a Conference* (Prentice-Hall, Inc., Englewood Cliffs, NJ), pp. 203–218.

- Camenen, B. & Larson, M. [2007] "A unified sediment transport formulation for coastal inlet application," Coastal and Hydraulics Laboratory Contract Report ERDC/CHL CR-07-1, U.S. Army Engineer Research and Development Center, Vicksburg, MS.
- Curtis, W. R., Hathaway, K. K., Seabergh, W. C. & Holland, K. T. [2001] "Measurement of physical model wave diffraction pattern using video," in *Proceedings 4th International Symposium of Ocean Wave Measurement and Analysis, Waves 2001, ASCE*, Vol. 1, pp. 23–32.
- Curtis, W. R., Hathaway, K. K., Holland, K. T. & Seabergh, W. C. [2002] "Video-based direction measurements in a scale physical model," Coastal and Hydraulics Laboratory Technical Note ERDC/CHL CHETN-IV-49, U.S. Army Engineer Research and Development Center, Vicksburg, MS.
- Demirbilek, Z., Lin, L. & Zundel, A. [2007] "WABED model in the SMS: Part 2. Graphical interface," Coastal and Hydraulics Laboratory Technical Note ERDC/CHL CHETN-I-74, U.S. Army Engineer Research and Development Center, Vicksburg, MS.
- Demirbilek, Z., Lin, L. & Nwogu, O. [2008] "Wave modeling for jetty rehabilitation at the Mouth of the Columbia River, Washington/Oregon, USA," Coastal and Hydraulics Laboratory Technical Report ERDC/CHL TR-08-xx (in review), U.S. Army Engineer Research and Development Center, Vicksburg, MS.
- Grunnet, N. M., Walstra, D. R. & Ruessink, B. G. [2004] "Process-based modelling of a shoreface nourishment," *Coastal Engineering* **51**(7), 581–607.
- Holthuijsen, L. H., Herman, A. & Booij, N. [2004] "Phase-decoupled refraction-diffraction for spectral wave models," *Coastal Engineering* **49**, 291–305.
- Isobe, M. [1998] "Equation for numerical modeling of wave transformation in shallow water," *Wave Phenomena and Offshore Topics, Chapter 3, Developments in Offshore Engineering*, ed. J. B. Herbich (Gulf Publishing Co., Houston, TX), pp. 101–162.
- Lin, L., Demirbilek, Z., Mase, H., Yamada, F. & Zheng, J. [2008] "A nearshore spectral wave processes model for coastal inlets and navigation projects," Coastal and Hydraulics Laboratory Technical Report ERDC/CHL TR-08-13, U.S. Army Engineer Research and Development Center, Vicksburg, MS.
- Lin, L. & Demirbilek, Z. [2005] "Evaluation of two numerical wave models with inlet physical model," *Journal of Waterway, Port, Coastal, and Ocean Engineering* **131**(4), 149–161.
- Lin, L., Mase, H., Yamada, F. & Demirbilek, Z. [2006] "Wave-action balance diffraction (CMS-Wave) model, Part 1: Tests of wave diffraction and reflection at inlets," Coastal Inlets Research Program Technical Note CIRP-TN-III-73, U.S. Army Engineer Research and Development Center, Vicksburg, MS.
- Longuet-Higgins, M. S. & Stewart, R. W. [1964] "Radiation stresses in water waves: A physical discussion with applications," *Deep-Sea Research* **11**, 529–562.
- Mase, H. [2001] "Multi-directional random wave transformation model based on energy balance equation," *Coastal Engineering Journal* **43**(4), 317–337.
- Mase, H. & Kitano, T. [2000] "Spectrum-based prediction model for random wave transformation over arbitrary bottom topography," *Coastal Engineering Journal* **42**(1), 111–151.
- Mase, H., Oki, K., Hedges, T. & Li, H. J. [2005] "Extended energy-balance-equation wave model for multidirectional random wave transformation," *Ocean Engineering* **32**, 961–985.
- Nwogu, O. & Demirbilek, Z. [2001] "BOUSS-2D: A Boussinesq wave model for coastal regions and harbors," Technical Report ERDC/CHL TR-01-25, Coastal and Hydraulics Laboratory, U.S. Army Engineer Research and Development Center, Vicksburg MS.
- Osborne, P. D. [2003] "Chapter 4, Oceanographic setting, field data collection, and analysis," Technical Report ERDC/CHL TR-03-12, Coastal and Hydraulics Laboratory, U.S. Army Engineer Research and Development Center, Vicksburg MS.
- Panchang, V. & Demirbilek, Z. [1998] "Wave prediction models for coastal engineering applications," *Wave Phenomena and Offshore Topics, Chapter 4: Developments in Offshore Engineering*, ed. J. B. Herbich (Gulf Publishing Co., Houston, TX), pp. 163–194.
- Penney, W. G. & Price, A. T. [1952] "The diffraction theory of sea waves by breakwaters and shelter afforded by breakwaters," *Philos. Trans. Roy. Soc. London Ser. A* **244**, 236–253.

- Pollock, C. E. [1995] "Effectiveness of spur jetties at Siuslaw River, Oregon; Report 2: Localized current flow patterns induced by spur jetties: Airborne current measurement system and prototype/physical model correlation," Coastal Engineering Research Center Technical Report CERC-95-14, U.S. Army Engineer Waterways Experiment Station, Vicksburg, MS.
- Rivero, F. J., Arcilla, A. S. & Carci, E. [1997a] "Implementation of diffraction effects in the wave energy conservation equation," presentation to *IMA Conf. on Wind-Over-Waves Couplings: Perspectives and Prospects*.
- Rivero, F. J., Arcilla, A. S. & Carci, E. [1997b] "An analysis of diffraction in spectral wave models," in *Proceedings 3rd Intl. Symp. of Ocean Wave Measurement and Analysis, Waves '97, ASCE*, pp. 431–445.
- Seabergh, W. C. [1988] "Observations on inlet flow patterns derived from numerical and physical model studies," *American Fisheries Society Symposium*, pp. 26–33.
- Seabergh, W. C. [1999] "Physical model for coastal inlet entrance studies," Coastal and Hydraulics Laboratory Technical Note IV-19, U.S. Army Engineer Research and Development Center, Vicksburg, MS.
- Seabergh, W. C. & Smith, J. M. [2001] "Wave scaling in tidal inlet physical models," in *3rd International Symposium on Ocean Wave Measurement and Analysis, ASCE*, pp. 228–237.
- Seabergh, W. C., Curtis, W. R., Thomas, L. J. & Hathaway, K. K. [2002] "Physical model study of wave diffraction-refraction at an idealized inlet," Coastal and Hydraulics Laboratory Technical Report ERDC/CHL-TR-02-27, U.S. Army Engineer Research and Development Center, Vicksburg, MS.
- Seabergh, W. C., Lin, L. & Demirbilek, Z. [2005a] "Laboratory study of hydrodynamics near absorbing and fully reflecting jetties," Coastal and Hydraulics Laboratory Technical Report ERDC/CHL-TR-05-8, U.S. Army Engineer Research and Development Center, Vicksburg, MS.
- Seabergh, W. C., Lin, L. & Demirbilek, Z. [2005b] "Laboratory measurements of waves and wave-induced currents at a jettied inlet," in *Proceedings 5th International Symposium on Ocean Wave Measurement and Analysis, Waves 2005, ASCE*, paper 131, pp. 1–10.
- Seabergh, W. C., Demirbilek, Z. & Lin, L. [2007] "Guidelines based on physical and numerical modeling for spur design at coastal inlets," *International Journal of Ecology and Development (IJED), Special Issue on Coastal Environments, Fall 2008* **11**(F08), 4–19.
- Sherwood, C. R., Gelfenbaum, G., Howd, P. A. & Palmsten, M. L. [2001] "Sediment transport on a high-energy ebb-tidal delta," in *Proceedings Coastal Dynamics '01, ASCE*, pp. 473–482.
- Smith, J. M., Resio, D. T. & Zundel, A. [1999] STWAVE: "Steady-state spectral wave model, Report 1, User's manual for STWAVE version 2.0," Coastal and Hydraulics Laboratory Instruction Report CHL-99-1, U.S. Army Engineer Waterways Experiment Station, Vicksburg, MS.
- Yu, Y.-X., Liu, S.-X., Li, Y. S. & Wai, O. W. H. [2000] "Refraction and diffraction of random waves through breakwater," *Ocean Engineering* **27**, 489–509.